The double capsules in macro-textured breast implants

Jean-Philippe Giot [a], Laurence S. Paek [a], Nathanael Nizard [a], Mostafa El-Diwany [a], Louis A. Gaboury [b], Monica Nelea [c], Joseph S. Bou-Merhi [a], Patrick G. Harris [a], Michel A. Danino [a, *]

[a] Division of Plastic Surgery, Department of Surgery, CHUM Montreal University Health Center, 1650 Sherbrooke East, Montréal, Québec H2L 4M1, Canada
[b] Institute for Research in Immunology and Cancer, Université de Montréal, C.P. 6128 succursale Centre-ville, Montréal, Québec H3C 3J7, Canada
[c] Institute of Biomedical Engineering, Department of Chemical Engineering, Ecole Polytechnique de Montréal, P.O. Box 6079, Station Centre-Ville, Montreal, Québec H3C 3A7, Canada

A R T I C L E   I N F O

A B S T R A C T

Breast implants are amongst the most widely used types of permanent implants in modern medicine and have both aesthetic and reconstructive applications with excellent biocompatibility. The double capsule is a complication associated with textured prostheses that leads to implant displacement; however, its etiology has yet to be elucidated. In this study, 10 double capsules were sampled from breast expander implants for in-depth analysis; histologically, the inner capsular layer demonstrated highly organized collagen in sheets with delamination of fibers. At the prosthesis interface (PI) where the implant shell contacts the inner capsular layer, scanning electron microscopy (SEM) revealed a thin layer which mirrored the three-dimensional characteristics of the implant texture; the external surface of the inner capsular layer facing the intercapsular space (ICS) was flat. SEM examination of the inner capsule layer revealed both a large bacterial presence as well as biofilm deposition at the PI; a significantly lower quantity of bacteria and biofilm were found at the ICS interface. These findings suggest that the double capsule phenomenon's etiopathogenesis is of mechanical origin. Delamination of the periprosthetic capsule leads to the creation of the ICS; the maintained separation of the 2 layers subsequently alters the biostability of the macro-textured breast implant.

© 2015 Elsevier Ltd. All rights reserved.

1. Introduction

1.1. Breast implant double capsules: definition and current controversy

An increasing number of reports have recently been published regarding double capsule formation around textured breast implants, mostly notably those with Biocell® type texturing [1]. The double capsule refers to the finding of 2 distinct capsular layers, separated by an intercapsular space (ICS), around an implant. The inner capsule is adherent to the prosthetic device at the prosthesis interface (PI) and the outer capsule to the surrounding sub-glandular/subcutaneous breast tissue [2]. Clinically, the respective surfaces of the inner and outer capsules that are in contact with the ICS are very smooth; variable amounts of seroma-like fluid can be found within the ICS. This double capsule phenomenon may be partial or complete. In the latter situation, double capsule formation appears around the entire prosthesis, rendering the implant particularly prone to micro-movements and dynamic malrotation due to the new, smoother interface between the inner and outer capsule layers. Consequently, the textured implant essentially acts as a smooth implant since the desired tissue in-growth into the textured surface and resultant implant stability are obviated [1,3]. Moreover, frictional forces between the 2 capsules may lead to development of synovial metaplasia, secondary infection and late seroma, thereby necessitating revision procedures [2]. The pathophysiology of double capsule formation is controversial; some authors propose a mechanical etiology while others suggest that normal periprosthetic fluid accumulation is the root cause [1,3–10].

* Corresponding author. Centre hospitalier de l'Université de Montréal, Hôpital Notre-Dame, 1560 rue Sherbrooke Est, Montréal, Qc H2L 4M1, Canada.
E-mail addresses: jp@giot.net (J.-P. Giot), laurence.paek@gmail.com (L.S. Paek), nizardnathanael@gmail.com (N. Nizard), mostafa.el-diwany@umontreal.ca (M. El-Diwany), louis.gaboury@umontreal.ca (L.A. Gaboury), Monica.nelea@polymtl.ca (M. Nelea), joseph.boumerhi@gmail.com (J.S. Bou-Merhi), patrick.harris.chum@ssss.gouv.qc.ca (P.G. Harris), daninoalain@gmail.com (M.A. Danino).

1.2. Biostability of breast implants

Breast implants are amongst the most widely used types of permanent implants in modern medicine and have both aesthetic and reconstructive applications. The biocompatibility of these prostheses is considered excellent and has been studied for over 50 years ever since their inception [11–13]. Still, numerous factors affect « capsule-implant » stability or biostability over time. Biostability of the expander implant device within the breast pocket helps prevent implant displacement and rotation, both of which may lead to undesirable greater expansion in the superior pole (subclavicular) or axillary regions [3,14]. For the round-shaped prosthesis, rotation in a plane parallel to the chest is only minimally discernable, but displacement over the rib cage from its intended position will result in a grossly abnormal appearance of the breast. In aesthetic and reconstructive surgery, implant stability is crucial to the overall success of the procedure; methods of monitoring implant biostability through 3D analyses have been recently proposed [15]. Currently, the most commonly utilized expander implants are anatomically shaped in the form of a teardrop in order to allow preferential expansion of the tissue in the lower pole of the breast envelope to better reestablish a natural breast shape. In such implants, malrotation and displacement leads to profound distortion of breast shape [3,16,17]. According to core studies performed by two of the principal breast implant manufacturers, asymmetry is the second leading cause of reoperation and was most commonly secondary to implant rotation or displacement. Capsular contracture was found to be the most frequent cause of reoperation [18,19].

1.3. The advent of breast implant texturation

To better stabilize the prosthesis on the thorax, manufacturers implemented implant texturation through modifications of the initially smooth silicone implant near the end of the manufacturing process. The Allergan Biocell® texturation, created by the "lost salt technique", is achieved by applying the implant shell with pressure onto a layer of fine salt. The Mentor Siltex® surface is made via negative contact imprinting from textured foam; the Siltex® surface is considered to be a less aggressive form of texturization than its Biocell® counterpart. Adherence is achieved by periprosthetic capsular tissue ingrowth into the pores of the textured shell surface, thereby essentially anchoring the silicone implant to the surrounding breast tissue. The senior author previously described the "Velcro effect" in which the periprosthetic capsule adheres to the implant surface in such a way that forceps are required in order to peel it off intraoperatively, hence simulating the feel of separating 2 actual Velcro surfaces apart [20]. The Velcro effect is typically observed with more aggressively textured implants.

1.4. Hypotheses

Based on the current literature, we propose 4 main hypotheses for the etiopathogenesis of double capsule formation (Fig. 1). The first hypothesis is based on movement of the prosthesis inside an oversized tissue pocket; the macro- and micro-movements of the implant prevents adhesion of the textured implant surface to the surrounding tissues [4]. The second hypothesis suggests a mechanical etiology whereby shear stress applied to the prosthesis–capsule complex pries the prosthesis away from the capsule; this separation leads to the subsequent creation of a new inner layer of capsule in direct contact with the prosthesis. As proposed by Hall-Findlay, continued friction between the textured implant shell and the original capsule leads to seroma-like fluid accumulation; secondary seeding of cells derived from this fluid onto the implant surface initiates the development of this new inner layer of adherent capsule [1,5]. The basis of the third hypothesis is that a seroma of varying etiology forms around the prosthesis, which subsequently leads to the development of a new inner capsule. The origin of the serous exudate could be infectious, allergic or hemorrhagic [6]. The fourth hypothesis is also mechanically based and proposes that shear forces cause detachment of the implant–capsule complex from the surrounding breast tissue, thereby leaving the original capsule en-bloc with the textured implant. Subsequently, a new outer capsule layer develops to produce the double capsule phenomenon [3,7,8].

1.5. Objectives

Using scanning electron microscopy, routine microbiology and histology, double capsule ultrastructural characteristics as well as the presence of biofilm and bacteria within both the PI and ICS were assessed in order to help elucidate the specific etiopathogenesis of this phenomenon.

2. Materials and methods

2.1. Definitions

As defined by Maxwell, the inner capsule is the membrane attached to the prosthesis. This inner capsule has 2 surfaces, one being at the interface with the prosthesis, referred to as the PI; the outer surface faces the space between the two capsules, referred to as the ICS. The separate and distinct outer capsule layer is adherent to the overlying breast tissue and also has two surfaces; the inner one is in contact with the ICS and the outer one is attached to the overlying muscle or breast parenchyma (Fig. 2) [2]. When the 2 distinct capsular layers do not envelope the entire implant, it is considered to represent a partial double capsule.

2.2. Patients

Following total mastectomy in breast cancer patients, approximately 90% of implant-based reconstructions are carried out in 2 stages [21]. In the first stage, a textured expander prosthesis is placed in the mastectomy breast pocket and placed underneath the thoracic muscles for partial to total coverage (pectoralis major muscle with or without serratus anterior muscle digitations). Postoperatively, after an initial wound healing period ranging from 2 to 6 weeks, the expander prosthesis is inflated with saline at regular intervals over the course of several weeks; once the desired breast mound volume is obtained, the expander is exchanged for a permanent silicone-filled prosthesis [22].

Ten patients with double capsule identified intraoperatively during second-stage expander to definitive implant exchange surgery were prospectively included in this study. Patients gave written consent for inclusion in this study, which was approved by the institutional review board. All included patients were treated at the same university hospital center by 1 of 4 plastic surgeons specialized in breast reconstruction. Baseline demographic data was collected for all patients and medical charts were reviewed for medical history, including radiotherapy status.

2.3. First-stage surgery: expander implant insertion

Prophylactic antibiotics were administered at induction (1st generation cephalosporin for 9 patients and clindamycin for 1 patient due to penicillin allergy). Skin prepping was performed using the standard solution of chlorhexidine with alcohol. Dissection of a submuscular plane under the pectoralis major muscle for expander
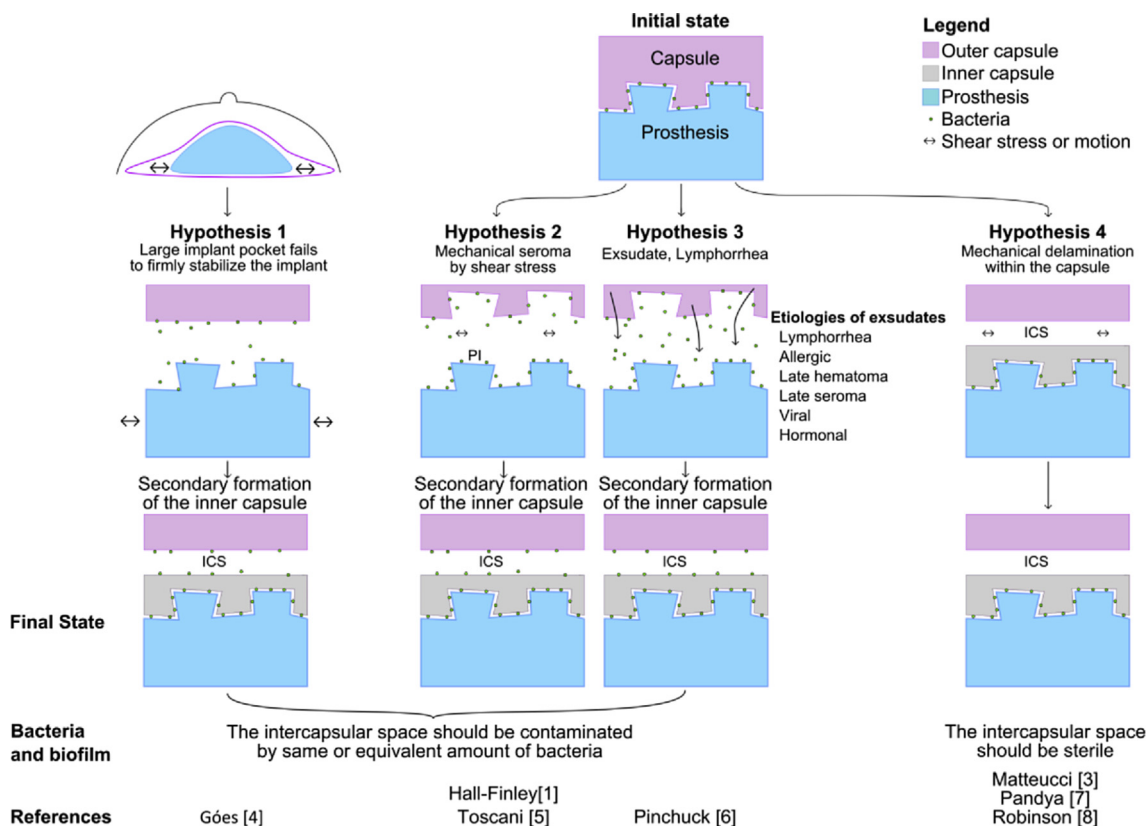
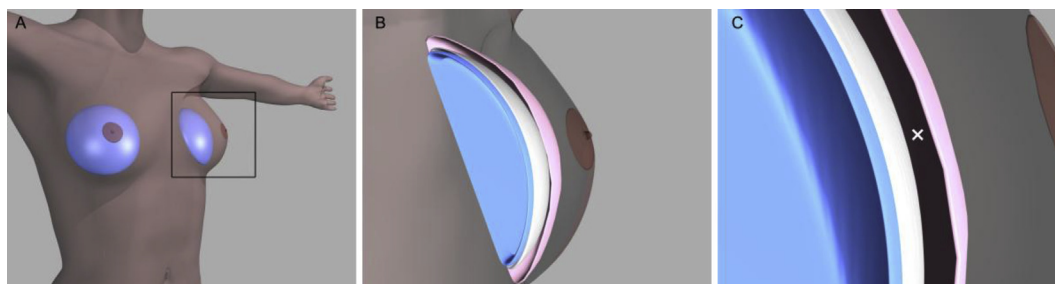**Fig. 1.** Illustration of proposed etiologies of double capsule formation.

Fig. 2. Artist's rendition of the breast prosthesis and periprosthetic capsules. A: Orientation of prosthesis placement in breasts. A close-up of the zone within the rectangular outline is presented in the second image. B and C: Breast capsule layers around the prosthesis. The prosthesis is in blue. The inner capsule is colored in gray and is firmly attached to the textured surface of the implant shell; the outer capsule is colored in pink. The area shaded in black (represented by white "x") represents physical space between the two capsule layers, referred to in article as the intercapsular space (ICS); the ICS may be filled with seroma-like fluid. (For interpretation of the references to colour in this figure legend, the reader is referred to the web version of this article.)

implant insertion was executed with electrocautery. Textured expander implants were inserted into the dissected pocket. Total muscle coverage of the expander device was achieved by adding a serratus anterior muscle flap in 7 cases. One case benefited from a latissimus dorsi muscle flap (patient #2) in order to achieve complete expander device coverage. Prior to insertion, all expander implants and breast pockets were bathed and irrigated with bacitracin antibiotic solution. Muscle closure was performed with absorbable suture. All surgeons installed 2 Jackson–Pratt drains (submuscular and subcutaneous planes) prior to 2-layered skin closure with absorbable sutures.

2.4. Second-stage surgery: definitive implant placement

Prior to the second-stage expander to definitive implant exchange procedure, the degree of capsular contracture in all patients

was assessed and graded according to the Baker scale [23]. The operative setup was the same as described in the first-stage procedure. Intraoperatively, during removal of the expander device, the surgeon documented the presence/absence of clinically observable Velcro effect and double capsule phenomenon. Two samples of 1 cm^2 of outer capsule were then biopsied at the level of the expander implant dome (most anterior and dependent portion) and the rib cage, respectively. For each sample, the capsule surface in contact with the ICS was subsequently tagged with a suture. It is important to note that these capsule samples were taken in a submuscular zone. A 9 cm^2 sample of the inner capsule layer together with its underlying segment of prosthesis shell was then biopsied *en-bloc*. The outer capsule and inner capsule/prosthesis samples were immediately fixed in a solution of glutaraldehyde 2% and sodium cacodylate 0.1 M in order to stabilize the cellular structures at a pH of 7.3. All samples were then stored in a

refrigerator at 4 °C for a minimum of 24 h. Capsule samples were analyzed as the study progressed. One sample of the inner capsule, one sample of the outer capsule and, if present, seroma-like fluid was collected by a swab; all were sent for aerobic and anaerobic bacterial cultures. Additional capsule samples were also sent for routine pathology.

2.5. Scanning electron microscopy (SEM)

The outer capsule was processed as previously described by our team; a 3 × 3 mm portion was cleaned, air-dried and gold-coated using an Agar Manual Sputter Coater for analysis under conventional High Vacuum (Hi-Vac) SEM [24]. The inner capsule was subsequently partially peeled from the adherent prosthesis shell in order to expose the PI and then cut into 2 parts to individually analyze both the PI and ICS surfaces; the same aforementioned processing methodology as the outer capsule sample was then employed (Fig. 3). Bacteria were identified as 0.2–2 μm cocci or bacilli-formed structures lying on the capsular surface. Bacteria density was reported as the bacteria count per analyzed surface (mm^2) of 2 observed fields shot at 3000X magnification.

Biofilm quantification was also assessed via SEM image observation at 3000X magnification. Two images for each sample were graded using the semi-quantitative biofilm scale of Van Heerden [25]. The means of the 2 obtained scores for each sample were then used for further analysis.

2.6. Colorization of scanning electron microscopy pictures

Using Photoshop software (Adobe, San Jose, California, USA), an area of interest was delineated and selected; in a new layer, colorization of the selected area was performed as follows: the prosthesis with 6292ff, bacteria with 18ff00, red blood cells with ff0000 and leukocytes with 4a96df (red, green and blue colors encoded in hexadecimal). The layers were merged with the original picture with a 30% transparency. No further modifications of photomicrographs were implemented.

2.7. Histology

Samples were sent for routine analysis to the pathology department of our institution. Paraffin blocks were sliced at 2 μm and subsequently stained by Hematoxyline Fluoxine Safran. Slides were scanned for further analysis on a NanoZomer Digital Pathology C9600 scanner and NDP Scan software (Hamamatsu).

2.8. Statistical analysis

Statistical analysis was performed using Graphpad Prism Software (La Jolla, California, USA). Wilcoxon matched pairs rank test was performed and α risk was defined at 1%. Outliers were determined using two-sided extreme studentized deviate test (Grubb's test) with α risk defined at 5%.

3. Results

Ten patients were included in this study. Eight patients underwent immediate breast reconstructions. The other 2 patients underwent delayed reconstructions, which took place 9.4 and 3.4 years post-mastectomy (patients #2 and #3, respectively). Mean patient age was 50.2 ± 4.9 and all were non-smokers. The double capsule was partial in 8 cases and complete in the 2 others; all double capsules were discovered fortuitously during the operations. All breast capsules were supple and were graded as Baker stages 1 or 2, therefore corresponding to a biocompatibility grade C of Steiert [13]. All expanders were from the same manufacturer Allergan with the 133 MV model being the most implanted, followed by the 133SX model, all these implants have a Biocell texturation. Two patients received radiotherapy. The first patient required adjuvant radiotherapy following mastectomy due to one close margin of tumor excision. This treatment delayed the second-stage expander to definitive prosthesis exchange procedure by a few months. Two months following the second-stage surgery, she presented with breast scar dehiscence and exposure of the underlying definitive implant, thereby leading to failure of the reconstruction. The second patient received radiotherapy 9.7 years prior to the mastectomy surgery. With the exception of the first patient, the postoperative courses after definitive implant placement were unremarkable.

Expanders received initial intraoperative inflations to 44 ± 22% of full volume capacity of the implant. Expansions began 25 ± 11 days postoperatively for a mean of 3.7 ± 1.4 weekly inflation sessions. The expander was exchanged for the definitive implant 175 ± 151 days after the last inflation session. Overall, the total timespan between the first- and second-stage surgeries (total time of expander prosthesis implantation) was 206 ± 124 days. These results are comparable to other studies we have previously reported [26]. Following routine analysis as per institutional protocol, cultures were negative for bacterial growth. However, it should be noted that the current routine cultures protocols in our institution may have insufficient sensitivity for the detection of a large part of the skin microflora as in the context of joint prostheses [27,28].

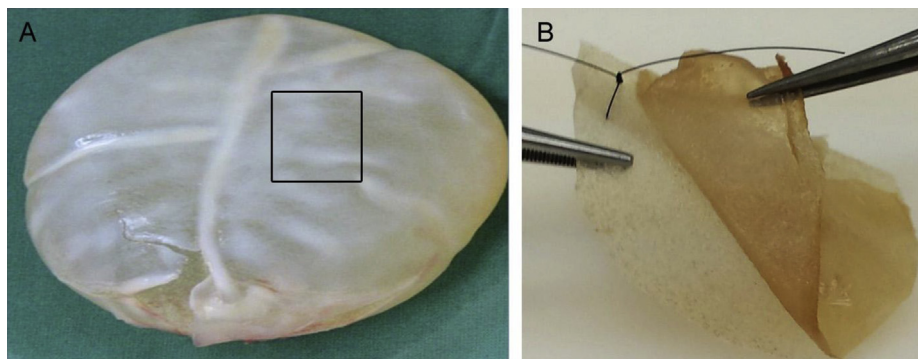Histologic analysis was performed on inner capsule samples and

Fig. 3. Peeling of the inner capsule. A: Double capsule covering the prosthesis. A 3 × 3 cm of inner capsule with prosthesis shell was sampled *en-bloc* (represented by the area within the black square). B: Using forceps, the inner capsule was partially peeled from left to right from the prosthesis shell in order to analyze ultrastructure of the prosthesis shell as well as inner capsule at both the prosthesis interface (PI) and intercapsular (ICS) surfaces.

analyzed thoroughly. The inner capsule samples were described as a superposition of thin sheets of organized collagen, lacking elastic fibers. Furthermore, the cell density of these inner capsules was minimal, and was comprised mainly of fibroblasts and few mononuclear cells. Interestingly, no blood vessels were identified. Intracapsular fractures parallel to the prosthesis surface and presenting as delamination of the inner capsule were observed in all specimens (Fig. 4).

On the contrary, the analysis of outer capsule samples demonstrated higher cellular density. Most cells were found on the ICS surface; furthermore, synovial metaplasia was observed in 70% of the cases. Collagen deposition was loosely organized with elastic fibers. The leukocytic infiltrate consisted mostly of lymphocytes, monocyte/macrophages and an extremely low number of granulocytes in the perivascular area. Granulocytes were identified occasionally within the vascular lumen but did not appear to leave the vasculature by diapedesis. Only 2 specimens showed hemosiderin deposits, which were limited to very small zones. Giant multinucleated cells surrounding silicon particles were observed in 5 specimens; these granulomas were embedded within the capsule.

Ultrastructural characteristics consistent with a clinical Velcro effect between the inner and outer layers of the periprosthetic capsule sheath were found in all cases; at the PI, the inner capsule predictably exhibited ingrowth into the prosthesis' textured surface rather than a simple adhesion. The outer aspect of the inner capsule (surface in contact with the ICS) presented a smooth surface with very little cellularity of either host or bacterial origin (Fig. 5A and B). The mean thickness of the inner capsule was 74.0 ± 29.7 μm and cross-sectional imaging of the inner capsule always revealed stratified organization of extracellular matrix (Fig. 5C). The SEM observation of the PI indicates that the inner capsule is extremely well anchored to the Biocell® texture (Fig. 5D and E). Once peeled

from the prosthesis, SEM observation of the PI aspect of the inner capsule layer revealed mirroring of the prosthesis texture (Fig. 5F). The outer capsule layer aspect in contact with the ICS demonstrated ultrastructural features that were identical to those of the adjacent outer aspect of the inner capsule; the surface was very smooth.

Bacterial cell density analysis at both the PI and ICS surfaces of the inner capsule revealed a large number of bacteria on the PI aspect (Fig. 6). On the ICS aspect of the inner capsule, a very low number of bacteria were found, except for in patient #1. The extreme studentized deviate test was significant; therefore, the first patient of this report was excluded from the statistical tests performed thereafter. The difference in bacterial density between the 2 surfaces of the inner capsule layer was statistically significant as illustrated in Fig. 7A (Wilcoxon rank test $p < 0.01$). The amount of bacterial biofilm within the PI and ICS of the double capsules was quantified using the van Heerden semi-quantitative scale and the results were then compared for each of the samples. Biofilm tended to cover a significantly larger area in the PI compared to the ICS as shown in Fig. 7B (Wilcoxon rank test $p < 0.01$).

4. Discussion

The increase in biocompatibility and stability of breast implants observed over the last decades has been largely due to the introduction of textured prosthetic devices [1]. We observed that bacterial load and biofilm presence was significantly lower or absent within the ICS, whereas bacteria could always be seen in the PI. This finding indicates that the PI and ICS were not sharing the same initial fluid, as would necessarily be the case in hypotheses 1, 2 and 3.

Also, the histology confirmed the layered appearance of the inner capsule and delamination that may occur within it. The inner capsule was the thinnest at the peaks of the prosthesis texture,
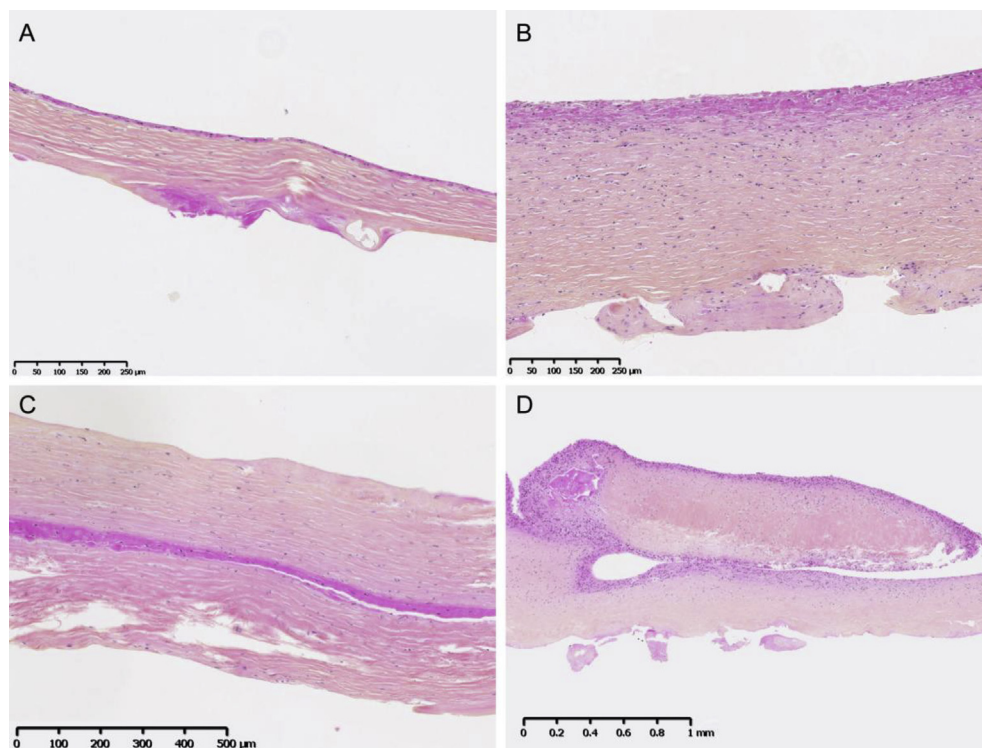

Fig. 4. Histological characteristics of the inner capsule. A, B: The inner capsule reveals variable thickness, between 65 and 475 μm. C, D: Intracapsular collagen fractures, presenting as delamination of the collagen, are located parallel to the implant surface. They are outlined by a discrete infiltrate of mononuclear cells, connecting to the intercapsular space (ICS) or to the prosthesis interface (PI). All images are oriented such that the ICS is located superiorly and the PI inferiorly.
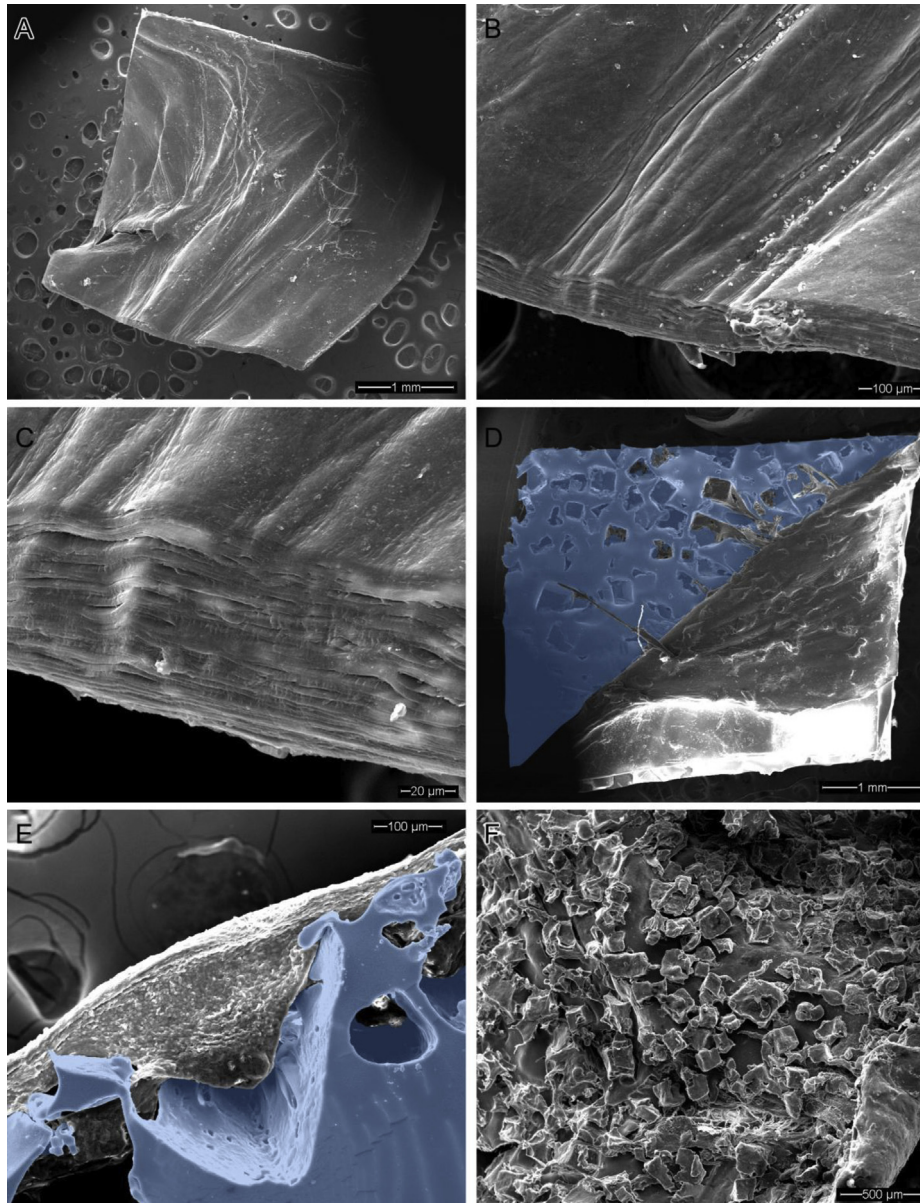
Fig. 5. Ultrastructural characteristics of the inner capsule. A and B: Outer aspect of the inner capsule in contact with the intercapsular space (ICS) C: Cross-sectional image showing the layered organization. D: Peeling of the inner capsule from the prosthesis surface revealing the Biocell® texture. The capsule is strongly adherent to the prosthesis and some degree of delamination within the capsular layer may take place, leaving some residual capsular tissue within the pores E: Cross-section section of the capsule segment remaining attached to the implant; the tissue ingrowth mirroring the prosthesis texture is demonstrated. D and E: prosthesis is colorized. F: Prosthesis interface (PI) aspect of the inner capsule demonstrating a near perfect mirror image of the corresponding implant shell texture seen in D.

which is consistent with the hypothesis that a mechanical shear stress delaminated the original capsule leaving an inner capsule that is thinned at the more mechanically solicited locations of the capsule.

Altogether, these findings support the 4th hypothesis, which advances the idea that double capsule formation is secondary to mechanical movement within the capsule. If the prosthesis was separated by any other way or if the seroma was secondary to the bacteria, then one would expect a similar distribution of bacteria in the PI and the ICS. Importantly, a resorbed hematoma would have left considerable long term hemosiderin deposits within the tissue. We only found extremely small hemosiderin deposits in 2 patients, thereby effectively excluding this etiology.

This research protocol allowed us to analyze capsules that matured from approximately 3 to 12 months. As for cutaneous and tendinous healing, the capsule is initially immature, consisting of loosely arranged collagen type III. As the collagen is progressively reorganized into collagen type I, the overall strength of the scar increases [29]. These double capsules were sampled at the conclusion of the first-stage expansion phase of prosthetic reconstruction, which indicates that the double capsule formation occurred during scar maturation and possibly evolved thereafter. This suggests that delamination of the immature capsule is a major factor contributing to early double capsule formation.

The routine bacterial cultures were negative despite large amounts of capsule sent for analysis. We found that most of the bacteria were embedded within bacterial biofilm, thereby indicating a hostile environment for bacteria. Biofilm further reduces the pathogens' susceptibility to host macrophage phagocytic action and also increases their resistance to systemic antibiotics. These
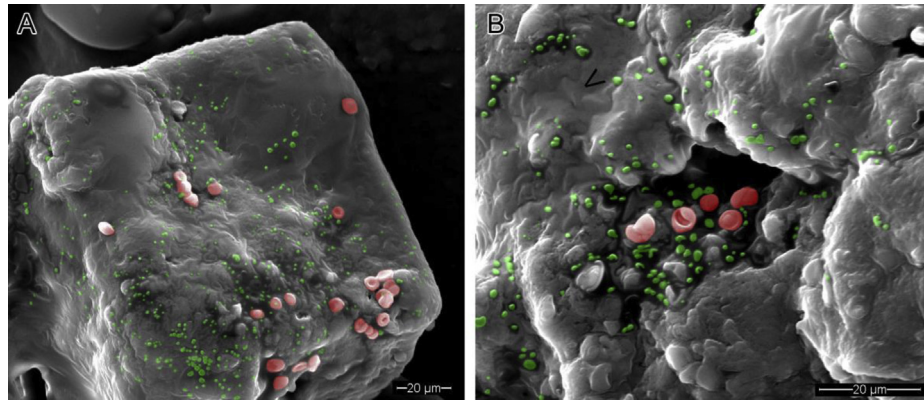
Fig. 6. Bacterial cell density quantification by SEM. A: Prosthesis interface (PI) aspect of the inner capsule, showing a mirror-image segment of capsular tissue ingrowth into the prosthesis texture pores covered by bacteria and red blood cells. B: Higher magnification image revealing bacteria surrounded by biofilm, depicted as "shadows" adjacent to the bacterial cells or like a thin wrinkled sheet covering the capsular tissue as indicated by the arrowhead (bacteria and red blood cells are colorized in green and red, respectively). (For interpretation of the references to colour in this figure legend, the reader is referred to the web version of this article.)
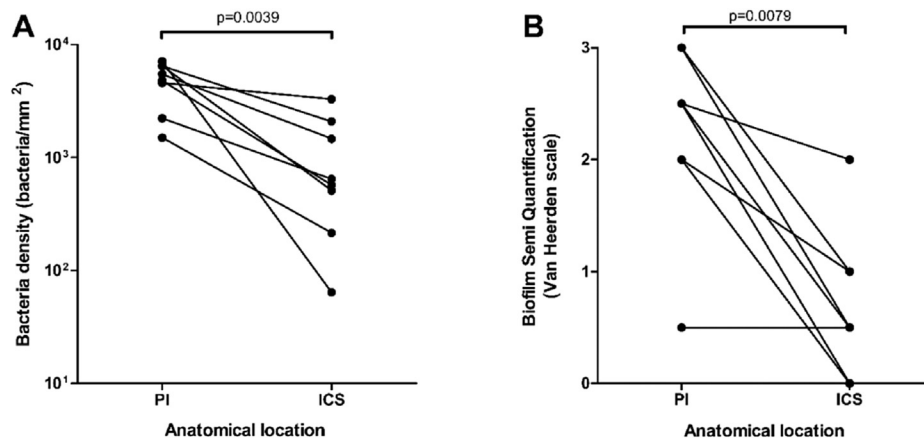

Fig. 7. Bacterial cell density and biofilm on the prosthesis interface (PI) and intercapsular Space (ICS) surfaces of the inner capsule. A: Bacteria were tallied on 2 images at 3000-fold magnification and mean bacterial density was used for statistical analysis (n = 9). B: Biofilm was quantified on 2 images per sample using the Van Heerden scale and represented as a mean of the 2 obtained measurements. Statistical analysis was performed using the Wilcoxon matched pairs test.

bacteria were most likely skin microbiome elements (Staphylococcus epidermidis, Propionobacterium acnes, Peptostreptococcus, etc.) which are difficult to isolate with conventional microbiology protocols [27]. Recent advances in biofilm disruption by sonication, prolonged cultures and polymerase chain reaction lead to improved bacterial detection around implants, which could be applied to overcome the limitations of standard techniques. Nevertheless, bacterial presence does not always have pathologic implications as the same microbes may be found in 20% of asymptomatic and supple capsules [30].

The case of patient #1 is interesting, as the radiotherapy occurred after the mastectomy and before the implant exchange. The scar breakdown is most likely principally secondary to radiotherapy effects, but might also be linked with the higher number of bacteria that were detected in the ICS. Further studies are required to analyze the specific impacts of radiotherapy and bacterial load.

Our group has shown that early inflation of expanders leads to an increased incidence of biofilm and double capsules with Biocell textured implants [31]. Other studies have demonstrated that when exposed to shear stress, bacteria adopt a different sessile phenotype that produces a more resistant biofilm [32,33]. These findings suggest that the biofilm formed within an environment exposed to the early shear stress of rapid implant expansion may be stronger due to a possible alteration in bacteria phenotype and other factors

yet to be elucidated. The gene secretion by bacteria as well as biofilm-modified immunogenicity may potentially trigger an altered response from the host immune system. Bacteria and leukocytes could therefore produce a different set of proteolytic enzymes that may weaken the immature capsule, thereby promoting intra-capsular delamination. In addition, Hu et al. have shown an increased quantity of bacteria and leukocytic infiltrate in contracted capsules of human breast textured prostheses, Biocell-textured implants having the highest load of textured implants [35]. These infiltrates may potentially contribute to the formation of double capsules particularly for Biocell-textured implants [1].

We observed that bacterial load and biofilm coverage differed on each side of a given double capsule sample. Future studies that compare the bacterial phenotypes and associated immune responses between the 2 double capsule surfaces, as well as with other textured and smooth implants, would further refine our understanding of the role of bacteria in double capsule pathogenesis.

The Biocell® macro-texturation clearly induces strong tissue ingrowth into its pores, which accounts for the exceptional stability of the capsule-implant complex. The weakest point is just above the peaks of the texture surface, where delamination occurs within 80 μm. On the contrary, less aggressively textured prostheses, such as the Mentor Siltex®, have a significantly reduced incidence of

double capsule, indicating a completely different capsular behavior and response to mechanical stress. Despite the reduced adherence to the prosthesis, these latter prostheses are still associated with reduced complication rates when compared to smooth implants [34]. We also think that in some cases, particularly with less aggressively textured implants, the mechanism of double capsule formation might be secondary to separation of the entire capsule and formation of an independent newer inner capsule (as in hypothesis 2). Our data are not sufficient to support hypothesis 2 and further studies on double capsules developing around textured implant shells other than the Biocell® type are needed.

5. Conclusion

Biostability is a critical aspect of the breast prosthesis. Double capsules lead to unfavorable clinical results; measures at both the manufacturing and clinical levels are essential to optimizing the proposed benefits of textured prostheses. Our study highlights the specific effects that aggressively textured breast implants may have on periprosthetic capsule formation and indicates that mechanical shear stress is one of the most important contributing factors to double capsule development.

Acknowledgments

References

[1] E.J. Hall-Findlay, Breast implant complication review: double capsules and late seromas, Plast. Reconstr. Surg. 127 (2011) 56—66.
[2] G.P. Maxwell, M.H. Brown, M.G. Oefelein, H.M. Kaplan, P. Hedén, Clinical considerations regarding the risks and benefits of textured surface implants and double capsule, Plast. Reconstr. Surg. 128 (2011) 593—595.
[3] P. Matteucci, L.R. Fourie, Double capsules related to dynamic malrotation of breast implants: a causal link? Br. J. Plast. Surg. 57 (2004) 289.
[4] J.C.S. Góes, A. Landecker, Optimizing outcomes in breast augmentation: seven years of experience with the subfascial plane, Aesthetic Plast. Surg. 27 (2003) 178—184.
[5] M. Toscani, et al., Breast implant complication: calcifications in the double capsule, Plast. Reconstr. Surg. 131 (2013) 462e—464e.
[6] V. Pinchuk, O. Tymofii, Seroma as a late complication after breast augmentation, Aesthetic Plast. Surg. 35 (2011) 303—314.
[7] A.N. Pandya, M.G. Dickson, Capsule within a capsule: an unusual entity, Br. J. Plast. Surg. 55 (2002) 455—456.
[8] H.N. Robinson, Breast implant complication review: double capsules and late seromas, Plast. Reconstr. Surg. 128 (2011) 818 author reply 818—819.
[9] D. Flassbeck, et al., Determination of siloxanes, silicon, and platinum in tissues of women with silicone gel-filled implants, Anal. Bioanal. Chem. 375 (2003) 356—362.
[10] R.J.I. Colville, N.R. McLean, P.A. Cross, True double capsules in oil-based (Trilucent) breast implants, Br. J. Plast. Surg. 55 (2002) 270—271.
[11] D.F. Williams, There is no such thing as a biocompatible material, Biomaterials 35 (2014) 10009—10014.
[12] Implants, C. On the S. of S. B. & Medicine, I. of. Safety of Silicone Breast Implants, National Academies Press, 2000.
[13] A.E. Steiert, M. Boyce, H. Sorg, Capsular contracture by silicone breast implants: possible causes, biocompatibility, and prophylactic strategies, Med. Devices Auckl. N. Z. 6 (2013) 211—218.
[14] J.L. Baeke, Breast deformity caused by anatomical or teardrop implant rotation, Plast. Reconstr. Surg. 109 (2002) 2555—2564 discussion 2568—2569.
[15] S.-P. Sun, K.-W. Hsu, J.-S. Chen, The stable status evaluation for female breast implant surgery by calculating related physics parameters, Comput. Methods Programs Biomed. 90 (2008) 95—103.
[16] W.P. Adams, Breast deformity caused by anatomical or teardrop implant rotation, Plast. Reconstr. Surg. 111 (2003) 2110—2111 author relply 2111—2112.
[17] T.S. Wilkinson, Rotation of anatomic breast implants, Plast. Reconstr. Surg. 112 (2003) 919—920 author reply 920.
[18] Center for Devices and Radiological Health & U.S. Food and Drug Administratin, FDA Update on the Safety of Silicone Gel-filled Breast Implants, 2011 at, http://www.fda.gov/downloads/MedicalDevices/ProductsandMedicalProcedures/ImplantsandProsthetics/BreastImplants/UCM260090.pdf.
[19] D.A. Caplin, J.M. Vargo, J. Canady, D. Hammond, Long-term clinical performance of memoryshape™ silicone breast implants in breast augmentation: prospective data through 9 years, Plast. Reconstr. Surg. 134 (2014) 92—93.
[20] A. Danino, F. Rocher, C. Blanchet-Bardon, M. Revol, J.M. Servant, A scanning electron microscopy study of the surface of porous-textured breast implants and their capsules. Description of the 'velcro' effect of porous-textured breast prostheses, Ann. Chir. Plast. Esthét. 46 (2001) 23—30.
[21] ASPS, 2012 Plastic Surgery Statistics Report, 2013 at, http://www.plasticsurgery.org/Documents/news-resources/statistics/2012-Plastic-Surgery-Statistics/full-plastic-surgery-statistics-report.pdf.
[22] Nava, M. B., Catanuto, G., Pennati, A., Visintini Cividin, V. & Spano, A. in (eds. Neligan, P., Warren, R. J. & Van Beek, A.) (Elsevier Saunders, 2013).
[23] J. Baker, Classification of Spherical Contractures, 1975.
[24] L.S. Paek, J.O. Tétreault-Paquin, S. St-Jacques, M. Nelea, M.A. Danino, Is environmental scanning electron microscopy a pertinent tool for the analysis of periprostethic breast capsules? Ann. Chir. Plast. Esthét. 58 (2013) 201—207.
[25] J. Van Heerden, M. Turner, D. Hoffmann, J. Moolman, Antimicrobial coating agents: can biofilm formation on a breast implant be prevented? J. Plast. Reconstr. Aesthet. Surg. 62 (2009) 610—617.
[26] A.M. Danino, et al., Comparison of the capsular response to the biocell RTV and mentor 1600 siltex breast implant surface texturing: a scanning electron microscopic study, Plast. Reconstr. Surg. 108 (2001) 2047—2052.
[27] P. Schäfer, et al., Prolonged bacterial culture to identify late periprosthetic joint infection: a promising strategy, Clin. Infect. Dis. Off. Publ. Infect. Dis. Soc. Am. 47 (2008) 1403—1409.
[28] M.E. Portillo, et al., Multiplex PCR of sonication fluid accurately differentiates between prosthetic joint infection and aseptic failure, J. Infect. 65 (2012) 541—548.
[29] S.M. Levenson, et al., Healing of rat skin wounds, Ann. Surg. 161 (1965) 293—308.
[30] U.M. Rieger, et al., Bacterial biofilms and capsular contracture in patients with breast implants, Br. J. Surg. 100 (2013) 768—774.
[31] L.S. Paek, et al., The impact of postoperative expansion initiation timing on breast expander capsular characteristics: a prospective combined clinical and scanning electron microscopy study, Plast. Reconstr. Surg. 135 (2015) 967—974.
[32] R.M. Donlan, J.W. Costerton, Biofilms: survival mechanisms of clinically relevant microorganisms, Clin. Microbiol. Rev. 15 (2002) 167—193.
[33] P. Stoodley, et al., The influence of fluid shear and AlCl3 on the material properties of Pseudomonas aeruginosa PAO1 and Desulfovibrio sp. EX265 biofilms, Water Sci. Technol. J. Int. Assoc. Water Pollut. Res. 43 (2001) 113—120.
[34] A. Araco, R. Caruso, F. Araco, J. Overton, G. Gravante, Capsular contractures: a systematic review, Plast. Reconstr. Surg. 124 (2009) 1808—1819.
[35] H. Hu, et al., Chronic biofilm infection in breast implants is associated with an increased T-cell lymphocytic infiltrate: implications for breast implant-associated lymphoma, Plast. Reconstr. Surg. 135 (2015) 319—329.